Eur. J. Mineral.
2008, **20**, 621–627
Published online May 2008

Kinetics of gypsum dehydration at reduced pressure: an energy dispersive X-ray diffraction study

MARILENA CARBONE[1,*], PAOLO BALLIRANO[2] and RUGGERO CAMINITI[3]

[1] Università di Roma Tor Vergata, Dipartimento di Scienze e Tecnologie Chimiche, Via della Ricerca Scientifica 1, 00133 Roma, Italy
*Corresponding author, e-mail: Marilena.Carbone@roma2.infn.it
[2] Sapienza Università di Roma, Dipartimento di Scienze della Terra, P.le A. Moro 5, 00185 Roma, Italy
[3] Sapienza Università di Roma, Dipartimento di Chimica, P.le A. Moro 5, 00185 Roma, Italy

Abstract: Gypsum ($CaSO_4 \cdot 2H_2O$) dehydration kinetics were investigated through energy dispersive X-ray diffraction (EDXD), under reduced pressure (100 Pa), in the temperature range 313–353 K. The process follows the JMAK (Johnson-Mehl-Avrami Kinetic) model. The fitting procedure of the Arrhenius expression provides an activation barrier of 18(2) kcal/mol. Under these experimental conditions, dehydration proceeds *via* a single-step conversion path gypsum → γ-anhydrite. Separate experiments of bassanite ($CaSO_4 \cdot 0.5H_2O$) dehydration, carried out at similar conditions, indicate, as expected, a faster process γ-anhydrite being the final product. According to the structural relationships between bassanite and γ-anhydrite, dehydration should occur *via* the escape of water molecules along the axis of the channel (*c* axis) following a one-dimensional behaviour. Therefore, no Avrami model (which implies nucleation and growth of a new phase) can be applied.

Key-words: gypsum, dehydration kinetics, bassanite, γ-anhydrite.

1. Introduction

The technological interest of calcium sulphates is related to the possibility of undergoing different hydration states, which inspired several scientific investigations. Within the $CaSO_4$-H_2O system, gypsum ($CaSO_4 \cdot 2H_2O$), bassanite (hemihydrate, $CaSO_4 \cdot 0.5H_2O$, which has also been reported as $CaSO_4 \cdot 0.67H_2O$) and β-anhydrite (insoluble anhydrite, β-$CaSO_4$) occur in nature as minerals. Much attention has been paid to the hydration-dehydration processes of calcium sulphates under various conditions, primarily for their application as binder. In fact, manufacture of plasters involves either calcinations or autoclaving of gypsum to form bassanite (or possibly an anhydrous form), followed by the addition of water to form a slurry which produces gypsum plaster on setting. For commercial use, bassanite is generally prepared by dehydration as it rarely occurs in nature (Yamamoto & Kennedy, 1969). Bassanite and γ-$CaSO_4$ (soluble anhydrite, γ-anhydrite) are low-temperature (T < 383 K) dehydration products of gypsum. γ-$CaSO_4$, a metastable phase which rapidly rehydrates under normal atmospheric conditions, converts to α-$CaSO_4$ at *ca.* 1500 K *via* a displacive transformation (Hanic *et al.*, 1985). Two forms of hemihydrate (α and β) are believed to exist showing different setting properties. At the present it is not clear if the two forms are characterized by different structures or if they differ only from a morphological and dimensional point of view. Moreover, various subhydrates with general formula $CaSO_4 \cdot nH_2O$ ($0.5 < n < 0.8$) have been reported (Bushuev & Borisov, 1982; Abriel, 1983; Kuzel & Hauner, 1987; Bezou *et al.*, 1995) but not adequately described. The low-temperature dehydration of gypsum has been investigated for many years. The first analysis of the process is attributed to Flörke (1952), which indicated a two-step process $CaSO_4 \cdot 2H_2O \rightarrow CaSO_4 \cdot 0.5H_2O \rightarrow$ γ-$CaSO_4$. An early study of the kinetics of dehydration of gypsum was performed, *in vacuo*, by Molony & Ridge (1968) whose results, based on X-ray powder diffraction, indicated that the process was best explained as a single step one, *i.e.* $CaSO_4 \cdot 2H_2O \rightarrow$ γ-$CaSO_4$. Subsequently Ball and coworkers (Ball & Norwood, 1969; Ball & Urie, 1970), using thermogravimetry, investigated both gypsum and bassanite dehydration processes at different vapour pressures and temperatures, determining the corresponding empirical activation energy E_a. More recently, an investigation carried out by neutron and X-ray powder diffraction (Abriel *et al.*, 1990) has indicated the occurrence of subhydrates $CaSO_4 \cdot nH_2O$ ($0 < n < 1$) during dehydration of gypsum. An almost simultaneous combined thermogravimetric and IR spectroscopy *in vacuo* study (Putnis *et al.*, 1990) indicated an apparently continuous water loss mechanism. According to those authors the reaction proceeds from gypsum to bassanite to γ-$CaSO_4$ without the occurrence of any further $CaSO_4 \cdot nH_2O$ ($0 < n < 0.5$ and $0.5 < n < 1$) intermediate-water-content form. The same behaviour

DOI: 10.1127/0935-1221/2008/0020-1826
0935-1221/08/0020-1826 $ 3.15

has been subsequently reported from thermo-Raman spectroscopy studies (Chang *et al.*, 1999). On the contrary, several recent papers have pointed out, from Raman and FTIR spectroscopic studies, a single-step dehydration process from gypsum to soluble anhydrite (Sarma *et al.*, 1998; Prasad, 1999; Prasad *et al.*, 2001, 2005). However at a pressure of 900 Pa a two-step process has been observed (Badens *et al.*, 1998), differently from the 1–500 Pa range. In a previous investigation (Ballirano *et al.*, 2001) carried out by our group, γ-anhydrite was produced by dehydration of gypsum at 423 K for one week. Subsequently, rehydration at room temperature as an effect of the air humidity (relative humidity RH *ca.* 30 %) was allowed, leading to the formation of $CaSO_4 \cdot 0.5H_2O$. This behaviour has been subsequently confirmed by other researchers (Chio *et al.*, 2004). Under these premises, we have undertaken an energy dispersive X-ray diffraction (EDXD) investigation on the kinetics of gypsum and bassanite dehydration, under reduced pressure, as a function of temperature in order to define and quantify the path of the process.

2. Experimental and methods

X-ray powder diffraction data were collected with a prototype of laboratory EDXD instrument (Caminiti *et al.*, 1991, 1997), characterized by vertical θ/θ geometry, and equipped with an environmental chamber. Detecting system is composed of an EG&G liquid-nitrogen-cooled ultrapure Ge solid-state detector ORTEC 92X linked to a multichannel analyzer. Calibration provided the relationship between energy E and channel number j which is linear and of the form $E = 0.0614\ j + 0.052$. Data were collected in symmetrical transmission mode (Wilson, 1973) because this instrumental setup is particularly convenient as all optical paths through the sample have the same length regardless of the depth of the scattering point from surface. Samples were prepared as pellets by pressing in a dye, at 4 t/cm^2 for 15 min, 200 mg of analytical-grade $CaSO_4 \cdot 2H_2O$ powder (ANALAR, product 10071). Bassanite was produced by spontaneous rehydration of γ-anhydrite produced by complete dehydration of gypsum. Phase identification was carried out by the Rietveld method on conventional angular dispersive X-ray diffraction (ADXD). Refinement provided structural data fully consistent with reference data (Ballirano *et al.*, 2001). Samples were placed within the environmental chamber fitted with a pumping system. Dynamic vacuum was kept constant to 100 Pa during the dehydration process. Temperature was controlled through an automatically driven copper heating support connected to a thermocouple immersed into the sample. For each sample, X-ray diffraction patterns were collected at room temperature, throughout the complete cycle of heating and while keeping the temperature constant at the set value. Gypsum dehydration experiments were carried out in the temperature range 313–353 K. In a typical run the pellet was inserted into the environmental chamber that was subsequently closed and evacuated. At this point the heating cycle was started under X-ray monitoring. As temperature reached the set value, counting time was started ($t = 0$). Spectra were collected with different counting times, depending on the temperature: those collected at low temperatures, corresponding to slower kinetic processes, permitted longer accumulation times. For temperatures exceeding 333 K collection time was reduced at the expenses of a lower signal/noise ratio. Typical collection times were of 250 s for T smaller than 333 K and 50 s for T greater than 333 K. Dead time never exceeded 7.5 % of accumulation time and it was subtracted from the overall counting time.

The dehydration process has been analyzed in terms of an almost constant density transition, *via* the collection of X-ray spectra as a function of time. A full derivation of the equations describing the scattered intensity in an EDXD experiment is reported in Caminiti & Rossi Albertini (1999). In a transition from phase ***1*** to phase ***2***, the progress of the dehydration reaction can be described in terms of fraction transformed $x(t)$ as a function of time using the relation:

$$x(t) = (I_{obs}(t) - I_{obs2})/(I_{obs1} - I_{obs2}) \quad (1)$$

where I_{obs} is the scattered intensity. I_{obs1} and I_{obs2} refer, respectively, to the spectra collected at $x = 0$ and $x = 1$ (*i.e.* before and after the transition). Equation (1) was applied directly to the total diffracted intensity during data analysis. In fact $x(t)$, at fixed θ, is a function of E, *i.e.* of the channel index j, since E and j are linked *via* a linear relation (see above). More details on the X-ray diffraction equipment used for the experiments are reported elsewhere (Caminiti *et al.*, 1999). In order to be considered a constant-density phase transition a few requirements should be fulfilled: *(i)* stoichiometry has to be constant throughout the transition; *(ii)* domains in each phase should be of dimensions such that the intradomain elastic scattered intensity shows the same spectral profile of a macroscopic object having an identical structure, *i.e.* surface effects must be negligible; *(iii)* elastic intensity of different domains should not mutually interfere. The dehydration process of gypsum occurs with loss of water and, as a consequence, it cannot be strictly speaking described as a constant density process. However, deviation from linearity can be evaluated from measurements in transmission geometry at $\theta = 0$. At this angle there is no diffraction but only absorption contribution, directly proportional to the mass of the sample. In a set of test measurements as a function of temperature and time, we were able to estimate that the deviation is of the order of 4 %.

3. Results and discussion

A preliminary analysis of the EDXD patterns was carried out to identify the diffractometric fingerprints of each phase occurring during the dehydration process, by comparison with reference calcium sulphates X-ray powder diffraction patterns (Ballirano *et al.*, 2001; Ballirano & Caminiti, 2001). Data collection was stopped well beyond the point where no further changes were observed in the patterns. A selection of spectra belonging to the data set collected at

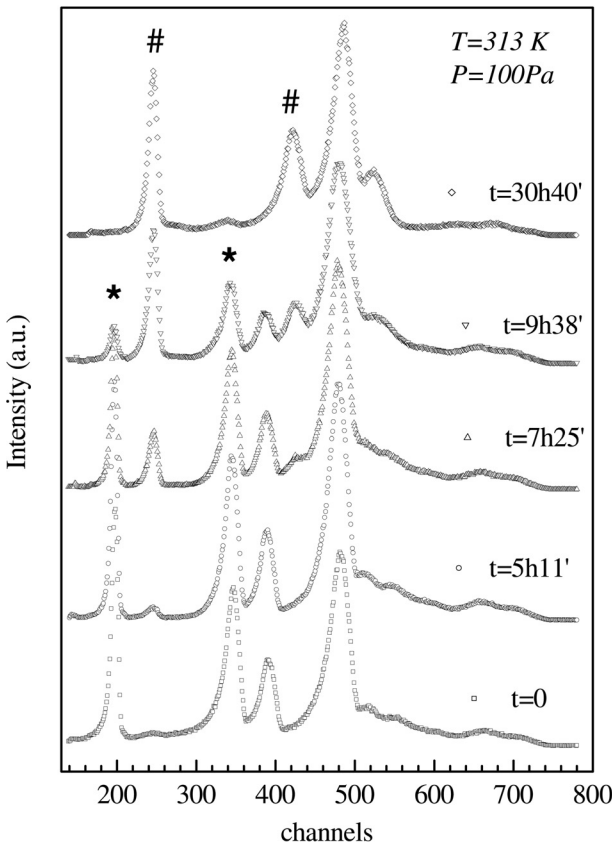

Fig. 1. Snapshots taken at different times of gypsum dehydration process at 313 K and 100 Pa. First spectrum (t = 0) corresponds to gypsum. Characteristic reflections of gypsum that do not overlap with those of dehydration phases are marked with a *. Non-overlapping reflections of dehydration products are marked, on the contrary, with a #. As a function of time, gypsum reflections disappear whereas those of dehydration products start to grow. Final dehydration product is γ-anhydrite ($CaSO_4$).

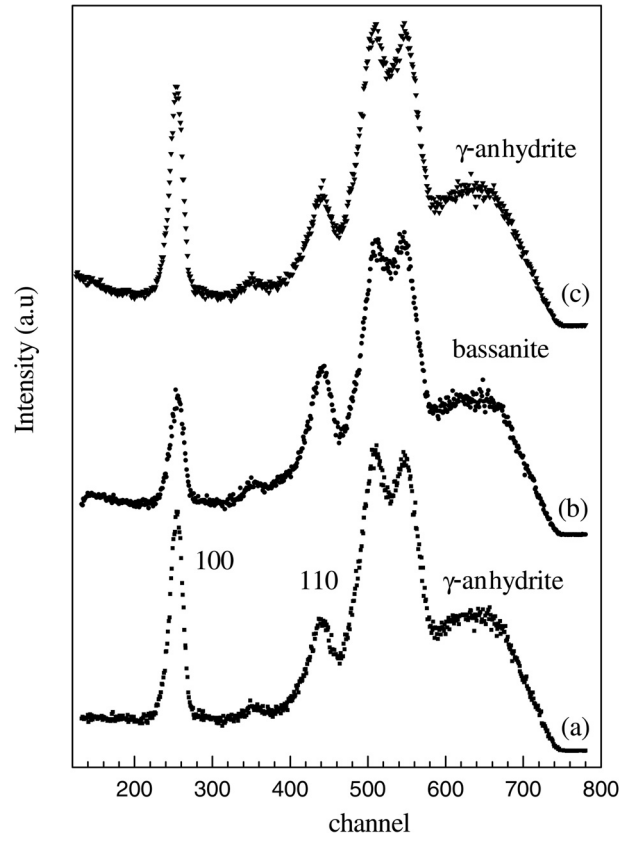

Fig. 2. γ-anhydrite-bassanite hydration and dehydration cycles. (a) γ-anhydrite obtained upon gypsum dehydration at 332 K and 100 Pa. (b) Re-hydration to bassanite after opening of the environmental chamber. (c) A further dehydration carried out at 333 K producing again γ-anhydrite.

313 K, taken at different t, is reported in Fig. 1. The nature of the final dehydration product was regularly checked by ADXD avoiding air exposure of the sample. Identification of characteristic diffraction peaks of gypsum was straightforward, at variance with the assignment of the diffraction effects to dehydrated phases, which was far more difficult, since the structural differences between γ-anhydrite and bassanite are relatively small. γ-anhydrite crystallizes in space group $P6_222$ (Lager *et al*., 1984; Ballirano *et al*., 2001) or possibly $C222$ (Bezou *et al*., 1985) ($a_{or} = \sqrt{3}\, a_{hex}$; $b_{or} = a_{hex}$; $c_{or} = c_{hex}$) a maximal non-isomorphic subgroup of $P6_222$. Bassanite is monoclinic $I2$ (Ballirano *et al*., 2001), strongly pseudo-trigonal, space group $P3_121$ (Abriel & Nesper, 1993). The reduction of symmetry for both compounds only results in the appearance of very weak extra reflections that are detectable in high-resolution experiments only. Moreover the basic sub-cells are similar (γ-anhydrite: a = 6.9694(8) Å, c = 6.3033(4) Å; hemihydrate: a = 6.937(2) Å, c = 6.345(1) Å) and the difference of the corresponding peaks position are small and not detectable with the present instrumental set-up. As a result, we were easily able to discriminate between reflections of gypsum and dehydrated phases, but we were not able to directly discriminate bassanite from γ-anhydrite. This holds mainly for the intermediate steps of the dehydration process, since the final dehydration product of each run was always γ-anhydrite. This was simply determined by opening the cell to air at the end of a dehydration run and monitoring the effects on the EDXD spectra (see Fig. 2). The effect of re-hydration was a reduction of the intensity ratio for the 100 and 110 reflections (indexing referred to the trigonal pseudo-cell of bassanite) from *ca.* 2:1 (γ-anhydrite) to 1:1 (bassanite), a behaviour in agreement with reference data (see Fig. 1 of Ballirano *et al*., 2001). In Fig. 1 peaks marked with a "*", indexed as 020 and 021, are characteristic of gypsum, without any interference with neighbouring reflections of dehydration products. Therefore, the area of these peaks can be directly related to the amount of gypsum present. Similarly, peaks marked with a "#", indexed as 100 and 110, were chosen as characteristic of both dehydration phases. Therefore, the dehydration process was analyzed by plotting the transformed fraction $x(t)$, derived from the integration of these peaks, against time. In particular 020 reflection of gypsum, within the channel range

$160 < j < 210$, and 100 reflection of dehydration products, within the channel range $210 < j < 270$, were selected. The process of γ-anhydrite re-hydration to hemihydrate and subsequent dehydration upon heating is shown in Fig. 2. Spectrum (a) refers to the final dehydration product obtained by heating gypsum at reduced pressure at 332 K. The intensity ratio between 100 and 110 is of *ca.* 2:1. The outcome was, then, exposed to air while collecting X-ray diffraction patterns and after a few minutes the re-hydration to bassanite was completed yielding spectrum (b). In this case the intensity ratio between 100 and 110 is of *ca.* 1:1. Moreover, dehydration of bassanite was subsequently carried out at 100 Pa and 333 K; γ-anhydrite was obtained again as final product as can be seen on spectrum (c).

As for possible presence and dehydration of bassanite $CaSO_4 \cdot 0.67H_2O$, it is only metastable and will disproportionate to $CaSO_4 \cdot 0.5H_2O$ and $CaSO_4 \cdot 2H_2O$. In $CaSO_4 \cdot 0.5H_2O$ every second possible water position is occupied, allowing a trigonal screw axis ($z(H_2O) \sim 0$, 1/3, 2/3), whereas in $CaSO_4 \cdot 0.67\ H_2O$ two of three possible H_2O-positions are occupied, destroying the trigonal screw axis found in γ-$CaSO_4$.

The kinetic aspects of gypsum dehydration were investigated at several temperatures in the 313–353 K range. For each spectrum of a given data set the transformed fraction $x(t)$ was calculated according to equation (1). Gypsum digestion was obtained from $x(t)$ calculated from the integrated intensity of 020 reflection as a function of time. Crystallization of dehydration phases was calculated from $x(t)$ calculated from the integrated intensity of 100 reflection as a function of time. Data were normalized in order to compare directly the behaviour of the two peaks. Plots of $x(t)$ *vs.* t, for the investigated temperatures, are reported in Fig. 3. Curves were vertically shifted relative to a final value $x(t) = 1.0$ in order to make them clearer.

As expected the onset of the dehydration process occurs faster as the temperature increases. The induction time for dehydration is 3 h at 313 K and is reduced to 30 min already at 321 K and to only 1 min at 353 K. Similarly, the reaction completion occurs earlier and earlier as a function of temperature, 11 h at 313 K and 30 min at 353 K. Careful scrutiny of the graphs indicates the presence of minor offsets between gypsum digestion (solid symbols in Fig. 3) and crystallization of dehydration products (open symbols in Fig. 3). There is a systematic displacement between the curves corresponding to dehydration phases crystallization and those corresponding to gypsum disappearance. This behaviour can be attributed either to the occurrence of minor errors in evaluating integrated intensities and/or to a contribution of the bassanite → γ-anhydrite conversion to the 100 reflection, as previously pointed out. The occurrence of a single or two-step process has been checked from evaluation of the dehydration phases 100 : 110 reflections intensity ratio. As can be seen from Fig. 1, the ratio 1:1 is never reached, not even at the first stages of the reaction. This clearly indicates that the dehydration proceeds *via* a single-step process gypsum → γ-anhydrite, under reduced pressure. The kinetics of such isothermal conversion was analyzed according to the so-called JMAK (Johnson, Mehl, Avrami Kinetics) model (Johnson & Mehl, 1939; Avrami, 1939; Avrami, 1940; Avrami, 1941) using the Avrami equation:

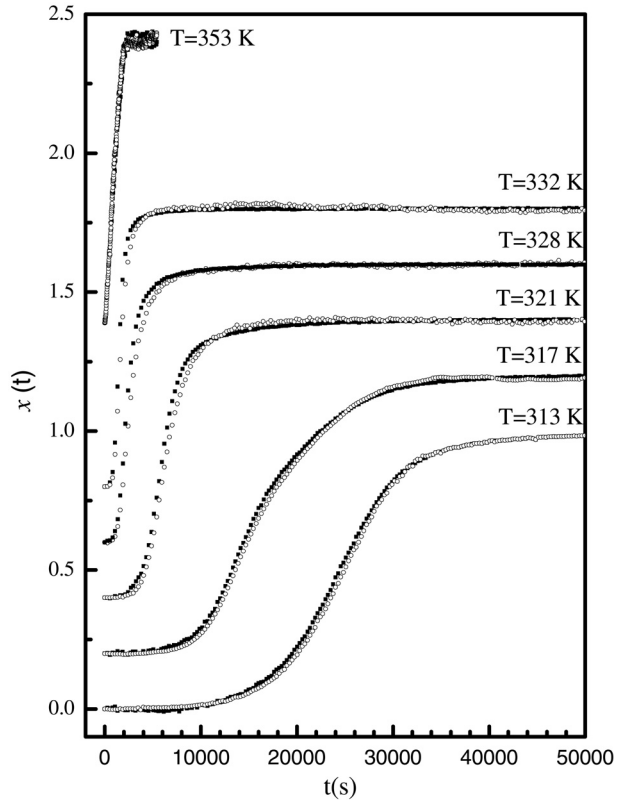

Fig. 3. Transformed fraction $x(t)$ of gypsum at 100 Pa as a function of time. Sigmoids were normalized and rigidly shifted vertically relative to a final value $x(t) = 1.0$ in order to increase readability. Solid symbol corresponds to $x(t)$ calculated from gypsum 020 reflection (represents the kinetics of gypsum disappearance). Open symbol corresponds to $x(t)$ calculated from dehydration phase 100 reflection (represents the kinetics of dehydration phase appearance).

$$x(t) = 1 - \exp[-kt^n] \qquad (2)$$

where k is a kinetic parameter depending on T, and the exponent n is related to the dimensionality of nucleation and growth. An example of the agreement between experimental and calculated data is shown in Fig. 4. Fitting parameters for the various data sets at different temperatures are reported in Table 1. The parameter n varies between 2.22 and 2.42, an indication that the growth process is a two-dimensional one. Kinetic parameters k were used, *via* the Arrhenius equation, to calculate the empirical activation energy E_a from the slope of the linear fit of the data in the plot of ln k as a function of $1/T$ (Fig. 5). We found an activation energy value of 18(2) kcal mol in fair agreement with 21.6 kcal mol^{-1} estimated by Putnis *et al.* (1990) from thermogravimetric and IR spectroscopy data, according to an apparently continuous water loss mechanism. However, a few differences between the two experimental set up should be mentioned. Those authors achieved a reduced water pressure by drying the atmosphere with a constant N_2 flow rate and used a ground fragment of a large

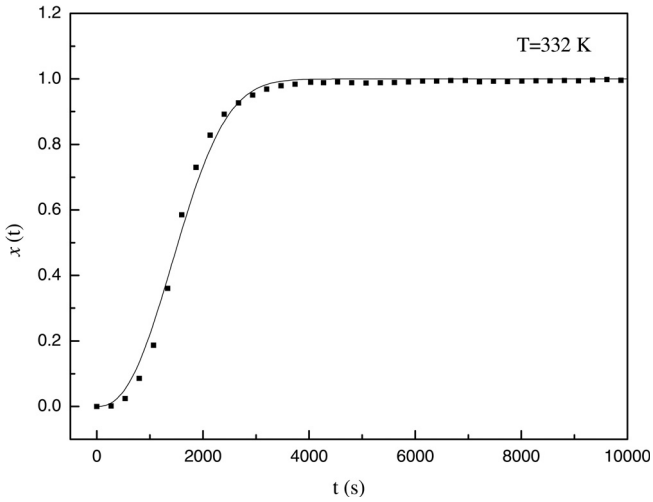

Fig. 4. Fitting of transformed fraction $x(t)$ *vs.* t with the Avrami model for the dehydration process at 332 K.

Table 1. Fitting parameters for the different data sets.

T (K)	k	n
313	1.4369×10^{-10}	2.22
317	4.3418×10^{-10}	2.23
321	1.7645×10^{-9}	2.28
328	7.9649×10^{-9}	2.34
332	1.5687×10^{-8}	2.40
353	1.1082×10^{-7}	2.42

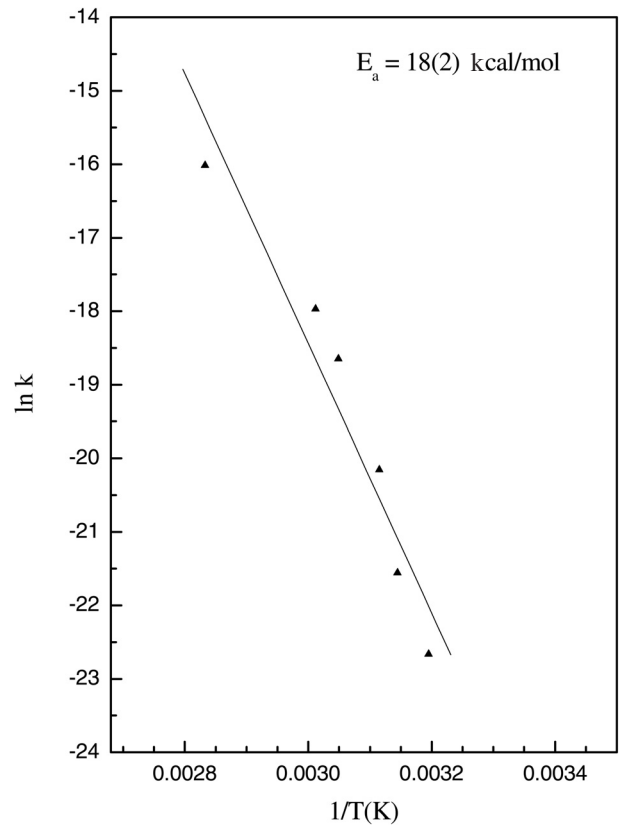

Fig. 5. Plot of ln k as a function of $1/T$. The slope of the linear fit provides the empirical activation energy E_a of gypsum dehydration.

natural single crystal as gypsum sample. Furthermore, they investigated the dehydration in a slightly different temperature range, *i.e.* 336–379 K.

Our value of E_a is in good agreement with the one reported by Ball & Norwood (1969) (*ca.* 19 kcal mol^{-1}), who also performed their experiments in similar conditions as ours (pressure, powder sample), though in a slightly higher temperature range, *i.e.* 353–425 K. They hypothesize a phase-boundary controlled mechanism, *i.e.* where the rate controlling step is the migration of the gypsum-hemihydrate interface.

The experiments of bassanite dehydration were carried out at 307, 316, 325, 333, and 341 K. The normalized curves $x(t)$ *vs.* t are reported in Fig. 6. Also in this case the curves were shifted vertically relative to a final value $x(t) = 1.0$ in order to increase readability. The process involves bassanite → γ-anhydrite conversion. A few aspects should be mentioned: *(i)* lack of the induction time; *(ii)* much faster completion time with respect to gypsum dehydration; *(iii)* curve shape cannot be properly fitted with the Avrami equation. The only significant structural difference between the two phases is the presence within the channels of water molecules that, in the case of bassanite, causes a small distortion of the structure (and therefore a symmetry reduction) through water molecules ordering. The common basic structural unit consists of chains of edge-sharing SO_4 tetrahedra and CaO_8 dodecahedra. These chains are arranged to form one-dimensional channels parallel to c axis. According to these features, dehydration of bassanite can be depicted like an evaporation process of water from the channels assisted by the reduced water pressure within the environmental chamber. In fact, according to the structural relationships between the two phases, dehydration should occur *via* the escape of water molecules along the axis of the channel following a one-dimensional behaviour. As a consequence, it does not need any nucleation, and in this sense, the Avrami model cannot be applied. This is similar, in many aspects, to the behaviour reported for nedocromil sodium tetrahydrate/monohydrate dehydration (Zhou *et al.*, 2003).

4. Conclusions

We have investigated by EDXD the kinetics of dehydration of gypsum ($CaSO_4 \cdot 2H_2O$) as a function of temperature in the range 313–353 K and at reduced water pressure. We found that gypsum dehydrates to γ-anhydrite (γ-$CaSO_4$) in a single-step process without the occurrence of bassanite as intermediate product. The overall process can be described through the Avrami model yielding an activation energy E_a of 18(2) kcal/mol. However, it is possible to obtain bassanite as stable phase, by re-hydrating γ-anhydrite. Bassanite dehydration occurs without the need of an induction time and is significantly faster than gypsum in similar conditions. In fact, according to the structural relationships

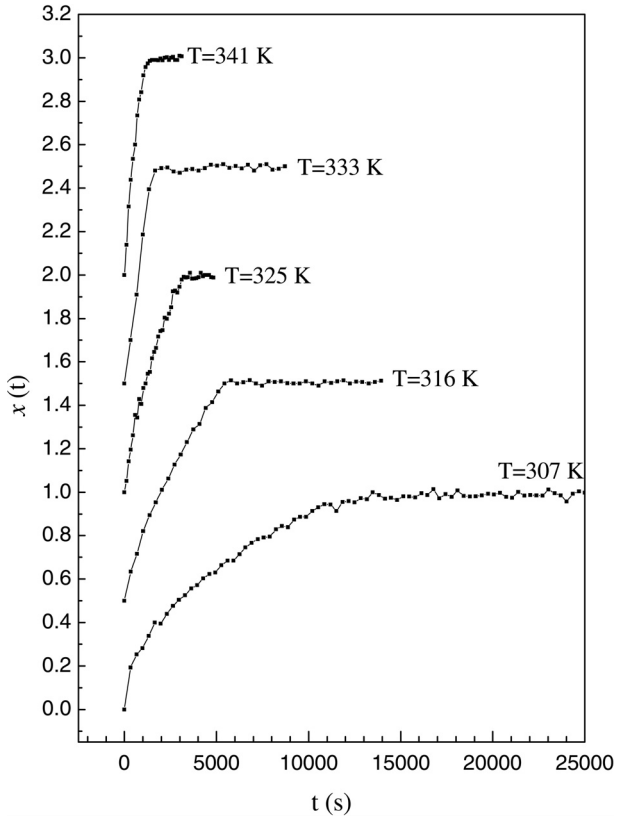

Fig. 6. Transformed fraction $x(t)$ of bassanite at 100 Pa as a function of time. Sigmoids were normalized and rigidly shifted vertically relative to a final value $x(t) = 1.0$ in order to increase readability.

between the two phases, dehydration should occur *via* the escape of water molecules along the *c* axis, following a one-dimensional behaviour. Therefore, the Avrami model (which implies nucleation and expansion of a new phase) is not adequate to describe the process.

References

Abriel, W. (1983): Calcium Sulfat Subhydrat, $CaSO_4 \cdot 0.8H_2O$. *Acta Cryst*., **C39**, 956-958.

Abriel, W. & Nesper, R. (1993): Bestimmung der Kristallstruktur von $CaSO_4(H_2O)0.5$ mit Röntgenbeugungsmethoden und mit Potentialprofil-Rechnungen. *Z. Kristallogr.*, **205**, 99-103.

Abriel, W., Reisdorf, K., Pannetier, J. (1990): Dehydration reactions of gypsum: A neutron and X-ray diffraction study. *J. Solid State Chem.*, **85**, 23-30.

Avrami, M. (1939): Kinetics of Phase Change. I. General Theory. *J. Chem. Phys.*, **7**, 11031112.

— (1940): Kinetics of Phase Change. II. Transformation-Time Relations for Random Distribution of Nuclei. *J. Chem. Phys.*, **8**, 212-224.

— (1941): Kinetics of Phase Change. III. Granulation, Phase Change, and Microstructure. *J. Chem. Phys.*, **9**, 177-184.

Badens, E., Llewellyn, P., Fulconis, J.M., Jourdan, C., Veesler, S., Boistelle, R., Rouquerol, F. (1998): Study of Gypsum Dehydration by Controlled Transformation Rate Thermal Analysis (CRTA). *J. Solid State Chem*., **139**, 37-44.

Ball, M.C. & Norwood, L.S. (1969): Studies in the system calcium sulphate–water. Part I. Kinetics of dehydration of calcium sulphate dehydrate. *J. Chem. Soc. A*, 1633-1636.

Ball, M.C. & Urie, R.G. (1970): Studies in the system calcium sulphate–water. Part II. The kinetics of dehydration of β-$CaSO_4$,$^1/_2H_2O$. *J. Chem. Soc. A*, 528-530.

Ballirano, P. & Caminiti, R. (2001): Rietveld refinements on laboratory energy dispersive X-ray diffraction (EDXD) data. *J. Appl. Cryst*., **34**, 757-762.

Ballirano, P., Maras, A., Meloni, S., Caminiti, R. (2001): The monoclinic *I*2 structure of bassanite, calcium sulphate hemihydrate ($CaSO_4 \cdot 0.5H_2O$). *Eur. J. Mineral*., **13**, 985-993.

Bezou, C., Nonat, A., Mutin, J.-C., Nørlund Christensen, A., Lehmann, M.S. (1995): Investigation of the Crystal Structure of γ-$CaSO_4$, $CaSO_4 \cdot 0.5\ H_2O$, and $CaSO_4 \cdot 0.6\ H_2O$ by Powder Diffraction Methods. *J. Solid State Chem.,* **117**, 165-176.

Bushuev, N.N. & Borisov, V.M. (1982): X-ray diffraction investigation of $CaSO_4 \cdot 0.67H_2O$. *Russ. J. Inorg. Chem*., **27**, 341-343.

Caminiti, R. & Rossi Albertini, V. (1999): Review on the kinetics of phase transitions observed by energy dispersive X-ray diffraction. *Int. Rev. Phys. Chem.*, **18**, 263-270.

Caminiti, R., Sadun, C., Rossi, V., Cilloco, F., Felici, R. (1991): Costruzione di un diffrattometro a raggi-X a dispersione di energia. Applicazioni su composti amorfi, liquidi e polveri cristalline. XXV National Congress of Physical Chemistry, Cagliari, Italy, June 17–21, 1991.

Caminiti, R., Sadun, C., Bionducci, M., Buffa, F., Ennas, G., Licheri, G., Musinu, A., Navarra, G. (1997): Energy dispersive X-ray diffraction applied to isothermal crystallization of the amorphous alloy $Ni_{60}B_{40}$. *Gazz. Chim. Ital*., **127**, 59-62.

Caminiti, R., Carbone, M., Panero, S., Sadun, C. (1999): Conductivity and Structure of Poly(ethylene glycol) Complexes Using Energy Dispersive X-ray Diffraction. *J. Phys. Chem.*, **103**, 10348-10355.

Chang, H., Huang, P.J., Hou, S.C. (1999): Application of thermo-Raman spectroscopy to study dehydration of $CaSO_4 \cdot 2H_2O$ and $CaSO_4 \cdot 0.5H_2O$. *Mater. Chem. Phys.*, **58**, 12-19.

Chio, C.H., Sharma, S.K., Muenow, D.W. (2004): Micro-Raman studies of gypsum in the temperature range between 9 K and 373 K. *Am. Mineral.*, **89**, 390-395.

Flörke, O.W. (1952): Kristallographische und röntgenometrische Untersuchungen im System $CaSO_4$-$CaSO_4 \cdot 2H_2O$. *N. Jb. Mineral. Abh.*, **84**, 189-240.

Hanic, F., Galikova, L., Havlica, J., Kapralic, I., Ambruz, V. (1985): Kinetics of the thermal decomposition of $CaSO_4$ in air. *Trans. J. Br. Ceram. Soc.*, **84**, 22-25.

Johnson, W.A. & Mehl, R.F. (1939): Reaction kinetics in processes of nucleation and growth. *AIME Trans.*, **135**, 416-420.

Kuzel, H.-J. & Hauner, M. (1987): Chemische und kristallographischeEigenschaften von Calciumsulfat-Halbhydrat und Anhydrit III. *Zement, Kalk, Gips Internaional*, **40**, 628-632.

Lager, G.A., Armbruster, T., Rotella, F.J., Jorgensen, J.D., Hinks, D.G. (1984): A crystallographic study of the low-temperature dehydration products of gypsum, $CaSO_4 \cdot 2H_2O$: hemihydrate $CaSO_4 \cdot 0.5H_2O$, and γ-$CaSO_4$. *Am. Mineral*., **69**, 910-918.

Molony, B. & Ridge, M.J. (1968): Kinetics of the dehydration of calcium sulphate dehydrate *in vacuo*. *Aust. J. Chem.*, **21**, 1063-1065.

Prasad, P.S.R. (1999): Raman intensities near gypsum-bassanite transition in natural gypsum. *J. Raman Spectr.*, **30**, 693-696.

Prasad, P.S.R., Pradhan, A., Gowd, T.N. (2001): *In situ* micro-Raman investigation of dehydration mechanism in natural gypsum. *Current Science*, **80**, 1203-1207.

Prasad, P.S.R., Krishna Chaitanya, V., Siva Prasad, K., Narayana Rao, D. (2005): Direct formation of the γ-$CaSO_4$ phase in dehydration process of gypsum: *In situ* FTIR study. *Am. Mineral.*, **90**, 672-678.

Putnis, A., Winkler, B., Fernandez-Diaz, L. (1990): *In situ* IR spectroscopic and thermogravimetric study of the dehydration of gypsum. *Mineral. Mag*., **54**, 123-128.

Sarma, L.P., Prasad, P.S.R., Ravikumar, N. (1998): Raman spectroscopic study of phase transitions in natural gypsum. *J. Raman Spectr.*, **29**, 851-856.

Yamamoto, H. & Kennedy, G.C. (1969): Stability relations in the system $CaSO_4$-H_2O at high temperatures and pressures. *Amer. J. Sci.*, **14**, 550-557.

Wilson, A.J.C. (1973): Note on the aberrations of a fixed-angle energy-dispersive powder diffractometer. *J. Appl. Cryst.*, **6**, 230-237.

Zhou, D., Schmitt, E.A., Zhang, G.G.Z., Law, D., Wight, C.A., Vyazovkin, S., Grant, D.J.W. (2003): Model-free treatment of the dehydration kinetics of nedocromil sodium trihydrate. *J. Pharm. Sci*., **92**, 1367-1376.

Received 7 August 2007
Modified version received 21 February 2008
Accepted 20 March 2008